The Plant Cell, Vol. 25: 1416–1429, April 2013, www.plantcell.org © 2013 American Society of Plant Biologists. All rights reserved.

BINDING PROTEIN Is a Master Regulator of the Endoplasmic Reticulum Stress Sensor/Transducer bZIP28 in *Arabidopsis*[C][W][OA]

Renu Srivastava,[a] Yan Deng,[a] Shweta Shah,[b] Aragula Gururaj Rao,[b] and Stephen H. Howell[a,c,1]

[a] Plant Sciences Institute, Iowa State University, Ames, Iowa 50011
[b] Roy J. Carver Department of Biochemistry, Biophysics, and Molecular Biology, Iowa State University, Ames, Iowa 50011
[c] Department of Genetics, Development, and Cell Biology, Iowa State University, Ames, Iowa 50011

BINDING PROTEIN (BiP) is a major chaperone in the endoplasmic reticulum (ER) lumen, and this study shows that BiP binds to the C-terminal tail of the stress sensor/transducer bZIP28, a membrane-associated transcription factor, retaining it in the ER under unstressed conditions. In response to ER stress, BiP dissociates from bZIP28, allowing it to be mobilized from the ER to the Golgi where it is proteolytically processed and released to enter the nucleus. Under unstressed conditions, BiP binds to bZIP28 as it binds to other client proteins, through its substrate binding domain. BiP dissociates from bZIP28 even when bZIP28's exit from the ER or its release from the Golgi is blocked. Both BiP1 and BiP3 bind bZIP28, and overexpression of either BiP detains bZIP28 in the ER under stress conditions. A C-terminally truncated mutant of bZIP28 eliminating most of the lumenal domain does not bind BiP and is not retained in the ER under unstressed conditions. BiP binding sites in the C-terminal tail of bZIP28 were identified in a phage display system. BiP was found to bind to intrinsically disordered regions on bZIP28's lumen-facing tail. Thus, the dissociation of BiP from the C-terminal tail of bZIP28 is a major switch that activates one arm of the unfolded protein response signaling pathway in plants.

INTRODUCTION

BINDING IMMUNOGLOBULIN PROTEIN, or simply Binding Protein (BiP), known in animal systems as 78-kD Glc-regulated protein or heat shock 70-kD protein 5, and calnexin/calreticulin are the two major chaperone systems in the endoplasmic reticulum (ER) lumen (Otero et al., 2010). BiP is primarily involved in the maturation and folding of nonglycosylated proteins (Hendershot, 2004). BiPs form complexes with the HSP40-like cochaperones containing J domains (ERdj3) and stromal-derived factor-2 (Jin et al., 2008; Nekrasov et al., 2009; Schott et al., 2010). These BiP complexes maintain nascent proteins in a competent state for subsequent folding and oligomerization (Anelli and Sitia, 2008).

BiP also plays an important role in the unfolded protein response (UPR) by regulating stress transducers, such as ACTIVATING TRANSCRIPTION FACTOR6 (ATF6), Protein kinase RNA-like ER kinase, and Inositol Requiring Enzyme1 (IRE1) in animal cells (Bertolotti et al., 2000; Shen et al., 2002). In response to stress, BiP and ATF6 rapidly dissociate, and ATF6 becomes a cargo in the ER-to-Golgi trafficking system (Shen et al., 2002). Shen et al. (2002) observed that BiP binds to three regions in the lumenal domain of ATF6. They reasoned that binding to these sites might mask Golgi localization signals (GLSs) on ATF6. They located the GLSs in two regions of the lumenal domain of ATF6 by showing that when these regions were deleted, transport of ATF6 to the Golgi and its processing by the Golgi-resident proteases were blocked. To demonstrate that BiP masked GLSs under unstressed conditions, they developed constructs in which the BiP binding sites were deleted, but putative GLSs were retained. These constructs were constitutively translocated to the Golgi, supporting the idea that BiP retains ATF6 in the ER by blocking its GLSs (Shen et al., 2002).

In plants, BiP is reported to play a role in the defense against various stresses. In particular, the overexpression of BiP in *Nicotiana tabacum* (tobacco) has been shown to protect against tunicamycin (TM) inhibition of seed germination and against water stress during plant growth (Alvim et al., 2001). When BiP was overexpressed in *Glycine max* (soybean), leaves of transgenic plants were more resistant to wilt and more tolerant of the loss of water potential than control plants when subjected to drought or osmotic stress (Valente et al., 2009). The greater stress resistance has been attributed to an attenuation of a cell death signal produced by ER and osmotic stress through N-RICH PROTEIN (NRP) and NAC6-mediated pathways (Reis et al., 2011). This implies that BiP is a negative regulator of stress-induced NRP-mediated cell death. In plants, BiP has also been shown to be a limiting factor in the folding of certain secreted proteins under ER stress conditions. Leborgne-Castel et al. (1999) reported that the production of α-amylase was reduced in a tobacco transient expression system subjected to ER stress but could be restored by cotransfection with *BiP*. *BiP2* loss-of-function mutants are defective PATHOGENESIS RELATED1 protein secretion in response

[1] Address correspondence to shh@iastate.edu.
The author responsible for distribution of materials integral to the findings presented in this article in accordance with the policy described in the Instructions for Authors (www.plantcell.org) is: Stephen H. Howell (shh@iastate.edu).
[C] Some figures in this article are displayed in color online but in black and white in the print edition.
[W] Online version contains Web-only data.
[OA] Open Access articles can be viewed online without a subscription.
www.plantcell.org/cgi/doi/10.1105/tpc.113.110684

to salicylic acid elicitation and are more susceptible to *Pseudomonas syringae* infection (Wang et al., 2005).

BiP plays a dual role in plant UPR. First, the genes encoding BiP are upregulated by the UPR. There are three BiP coding genes in *Arabidopsis thaliana*, and *BiP3*, in particular, is most highly upregulated by abiotic stress or by ER stress agents (Koizumi, 1996; Martínez and Chrispeels, 2003; Iwata and Koizumi, 2005; Liu et al., 2007b; Iwata et al., 2008, 2010; Tajima et al., 2008; Liu and Howell, 2010). Since BiP is a chaperone, it is thought to mitigate stress by binding to misfolded proteins in the ER, preventing their aggregation during refolding processes. Second, BiP is thought to regulate the activity of the ER stress sensor/transducers, bZIP17 and bZIP28, plant homologs of mammalian ATF6 and related factors. bZIP17 and bZIP28 like ATF6 are membrane-associated transcription factors activated by various stresses in a process that involves their mobilization from the ER to the Golgi where they are processed and released by site 1 and site 2 proteases (S1P and S2P) (Liu et al., 2007a, 2007b).

In this study, we examined the role of BiP in retaining bZIP28 in the ER under unstressed conditions and allowing it to mobilize to the nucleus in response to stress to upregulate target genes. BiP binds to the C-terminal, lumen-facing tail of bZIP28, and in response to ER stress, BiP dissociates from bZIP28, releasing it from the ER. The deletion of the bZIP28 C-terminal tail prevents bZIP28's retention in the ER under unstressed conditions and allows it to relocate to the nucleus to constitutively upregulate stress response genes.

RESULTS

BiP Binds to bZIP28 under Unstressed Conditions

BiP binds to bZIP28 in unstressed *Arabidopsis* seedlings as demonstrated by the coimmunoprecipitation of BiP with myc-bZIP28 in transgenic lines expressing myc-bZIP28 (Figure 1A). *Arabidopsis* encodes three BiP isoforms, BiP1 to BiP3, that are predicted to be ER lumenal proteins (see Supplemental Figure 1 online). The anti-BiP antibody used in these studies does not discriminate between the BiPs. Therefore, to determine which isoforms of BiP bind to bZIP28, we FLAG-tagged BiP1 and BiP3 and used the epitope-tagged forms in immunoprecipitation experiments with myc-bZIP28 transiently expressed in *Nicotiana benthamiana* leaves. BiP2 was not used in these experiments because BiP1 and BiP2 are nearly identical in sequence (see Supplemental Figure 1 online). We observed that both BiP1-flg and BiP3-flg coimmunoprecipitate with myc-bZIP28 (Figure 1B). We were also able to pull down myc-bZIP28 using BiP antibodies from unstressed *Arabidopsis* plants (see Supplemental Figure 2 online). These results confirmed that bZIP28 does indeed interact with BiP.

Characteristics of BiP Binding to bZIP28

We performed further experiments to determine the characteristics of BiP binding to bZIP28. BiP appears to bind myc-bZIP28 as it does to other client proteins. BiP coimmunoprecipitated

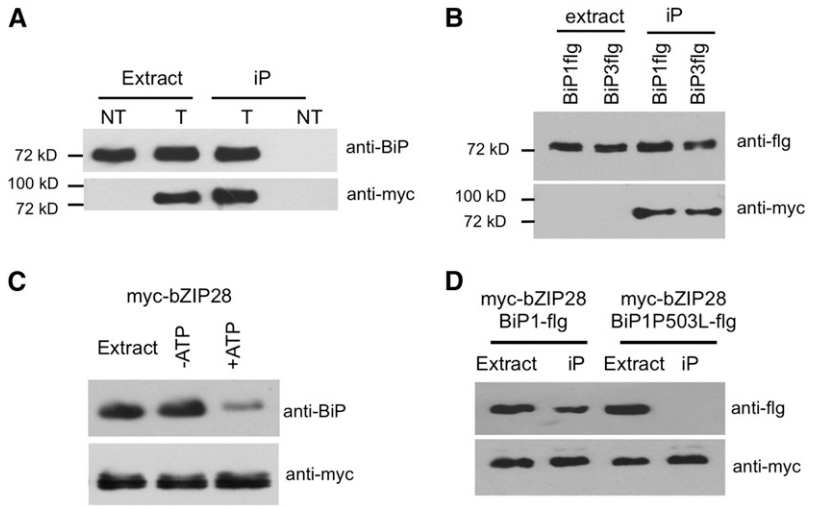

Figure 1. BiP Binds to bZIP28.

(A) myc-bZIP28 was detected in extracts and immunoprecipitates (iP) from of roots of unstressed 7-d-old transgenic (T) and nontransgenic control (NT) *Arabidopsis* seedlings. Immunoblots were probed with anti-BiP and anti-myc antibodies. The anti-BiP antibody that was used for immunoprecipitations did not bind to agarose beads alone.

(B) Both BiP1-flg and BiP3-flg bind to myc-bZIP28. myc-bZIP28 was immunoprecipitated from extracts of *N. benthamiana* leaves transiently expressing BiP1-flg and BiP3-flg. Immunoblots were probed with anti-flg and anti-myc antibodies.

(C) BiP bound to myc-bZIP28 extracted from myc-bZIP28 expression lines is released by ATP. myc-bZIP28 was immunoprecipitated with anti-myc antibodies and incubated for 30 min with or without 2 mM ATP and 2 mM $MgCl_2$. Immunoblot was probed with anti-BiP and anti-myc antibodies.

(D) Mutant BiP with a defect in substrate binding does not bind bZIP28. myc-bZIP28 coexpressed with BiP1-flg or BiP1P503L-flg in the transient expression system was immunoprecipitated with anti-myc antibodies. Immunoblot was probed with anti-flg and anti-myc antibodies.

with carboxypeptidase Y star–green fluorescent protein (CPY*-GFP), a known BiP substrate (Izawa et al., 2012), when it was expressed from a transgene in *Arabidopsis* (see Supplemental Figure 3 online). Client proteins can be released from BiP by ADP/ATP exchange in BiP's N-terminal nucleotide binding domain (Wei et al., 1995). BiP was released from myc-bZIP28 upon incubation of the immunoprecipitate with ATP and $MgCl_2$ and was not released in the absence of ATP (Figure 1C). In addition, BiP did not bind to myc-bZIP28 when BiP's substrate binding domain was disabled by substituting Pro at position 503 for Leu. In mammalian systems, the equivalent substitution of a Pro for Leu at position 495 (BiPP495L) gives rise to a form that is defective in substrate binding (Shen et al., 2005). When *Arabidopsis* BiP1P503L-flg was expressed along with myc-bZIP28, -BiP1P503L-flg did not coimmunoprecipitate with myc-bZIP28 (Figure 1D). Thus, we concluded that under unstressed conditions, BiP binds to bZIP28 similarly to the manner in which BiP binds to other client proteins.

BiP Dissociates from bZIP28 under Stress

When seedlings are treated with ER stress agents, such as TM, bZIP28 is transported from the ER to the nucleus via the Golgi apparatus (Liu et al., 2007b; Srivastava et al., 2012). We were interested in determining whether BiP dissociates from bZIP28 in response to stress and whether the dissociation of BiP is correlated with other events involved in the mobilization of bZIP28. Therefore, we performed coimmunoprecipitations of myc-bZIP28

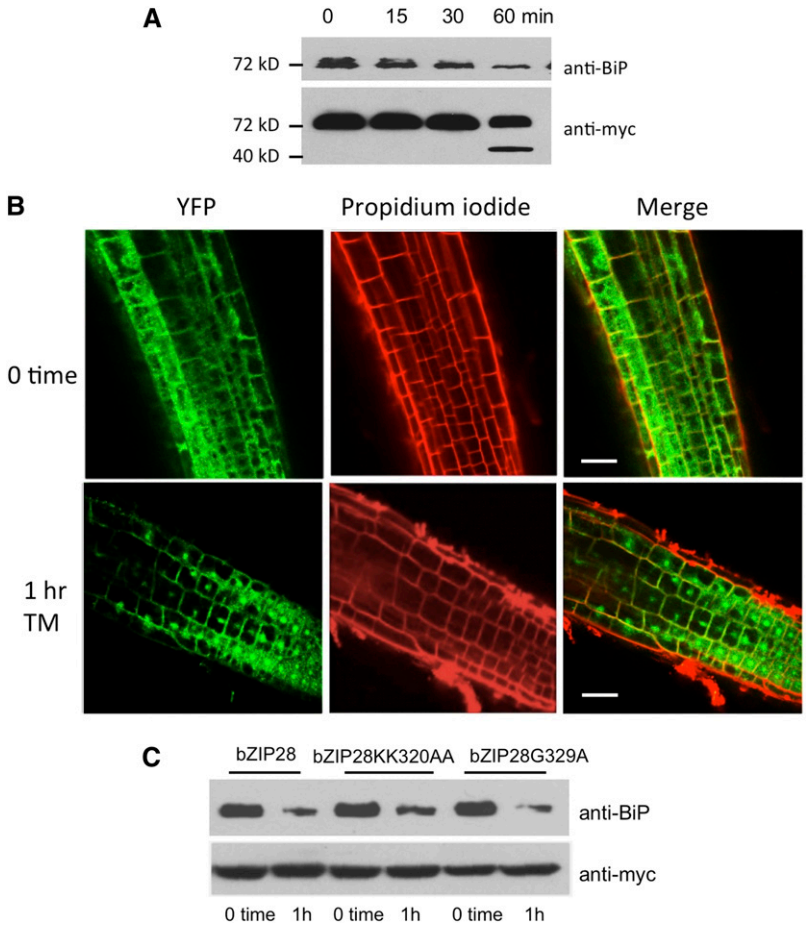

Figure 2. BiP Dissociates from bZIP28 in Response to ER Stress.

(A) Seven-day-old *Arabidopsis* seedlings expressing myc-bZIP28 were treated with 2 μg/mL TM, and proteins were extracted (from whole seedlings) at times indicated following TM treatment. Extracts were immunoprecipitated with anti-myc antibodies, and immunoblot was probed with anti-BiP and anti-myc antibodies. The fast migrating band visualized by the anti-myc antibody is the proteolytically processed form of myc-bZIP28.

(B) Confocal images of roots of *Arabidopsis* seedlings expressing YFP-bZIP28. Seedlings were treated for 1 h with 2 μg/mL TM. Roots were stained with propidium iodide to show cell outlines. Bars = 50μm.

(C) BiP dissociates in response to stress from mutant forms of bZIP28 that are prevented from exiting the ER or from being released from Golgi bodies. Seven-day-old *Arabidopsis* expressing various forms of myc-bZIP28 were treated with TM for 1 h, and proteins were extracted, immunoprecipitated with anti-myc, subjected to immunoblot analysis, and probed with anti-BiP and anti-myc antibodies. bZIP28KK320AA is blocked in exiting the ER, and bZIP28G329A is not proteolytically cleaved by S2P and therefore is not released from Golgi bodies.

and BiP during a time course of movement of bZIP28 from the ER to the nucleus as described by Srivastava et al. (2012). BiP progressively dissociated from myc-bZIP28 during an hour after treating seedlings with TM (Figure 2A; see Supplemental Figure 2 online). The loss of BiP from myc-bZIP28 immunoprecipitates was due to dissociation and not to degradation of BiP because BiP levels did not decline during the time course of these experiments (see Supplemental Figure 4 online). At ~30 min after the start of stress treatment, bZIP28 begins to exit the ER (Srivastava et al., 2012), and by 1 h, myc-bZIP28 was being proteolytically processed (Figure 2A) and yellow fluorescent protein (YFP)-bZIP28 appeared in the nucleus (Figure 2B; see Supplemental Figure 5 online). Since BiP dissociation and YFP-bZIP28 movement occurred at about the same time, we asked whether the dissociation of BiP depends on exit of bZIP28 from the ER. To do so, we looked for the dissociation of BiP from myc-bZIP28KK320AA, a mutant that is incapable of exiting the ER. bZIP28KK320AA has an altered pair of Lys residues on the cytoplasmic side of the membrane, which impedes its interaction with COPII vesicle components and its exit from the ER (Srivastava et al., 2012). BiP bound to myc-bZIP28KK320AA under unstressed conditions and dissociated from it following TM treatment (Figure 2C). Since it takes about an hour of TM treatment for most of BiP to dissociate from wild-type myc-bZIP28, the question can be asked whether the

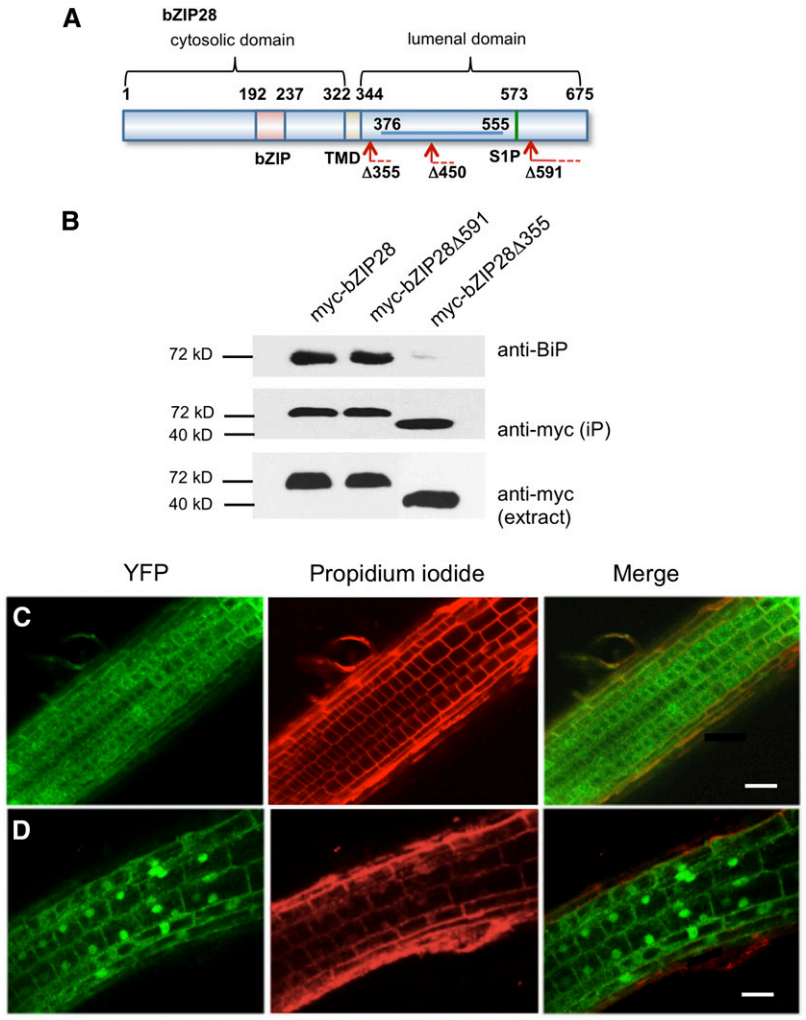

Figure 3. The Effect of Truncations on bZIP28 Mobilization.

(A) Map shows truncations in myc-bZIP28 and the region of the protein (blue line) that was used in the phage display analysis.

(B) Coimmunoprecipitation experiments of BiP with truncated forms of bZIP28. Proteins were extracted from 7-d-old *Arabidopsis* seedlings expressing myc-tagged forms of the truncated constructs myc-bZIP28Δ591 and myc-bZIP28Δ355 and subjected to immunoblot analysis probed with anti-BiP and anti-myc antibodies. The expression levels of truncated forms of the myc-bZIP28 constructs in the lines used are shown in the crude protein extracts [labeled anti-myc (extract)].

(C) Subcellular localization of YFP-bZIP28Δ591 in root cells under unstressed conditions.

(D) Relocation of YFP-bZIP28Δ591 to nuclei in root cells of seedlings treated with 2 μg/mL TM for 1 h. Confocal images of *Arabidopsis* roots counterstained with propidium iodide to show cell outlines. Bars = 50 μm.

dissociation is only apparent because the myc-tagged N terminus of bZIP28 is cleaved off in the Golgi. To test this, we determined whether BiP dissociated from myc-bZIP28G329A, a form of bZIP28 that has a mutation in its transmembrane domain, making it resistant to proteolytic cleavage by S2P and incapable of being released from the Golgi (Srivastava et al., 2012). BiP dissociated from myc-bZIP28G329A following TM treatment (Figure 2C). Therefore, BiP dissociates from bZIP28 in response to ER stress whether or not its exit is blocked from either the ER or Golgi.

BiP Binding Retains bZIP28 in the ER

To test whether BiP retains bZIP28 in the ER by binding to bZIP28's C-terminal tail, two major truncation constructs were developed: YFP-bZIP28Δ591, which eliminated most of the C terminus downstream of the S1P site; and YFP-bZIP28Δ355, which removed most of bZIP28's C-terminal tail residing in the ER lumen (Figure 3A). We tested these truncations of bZIP28 for their ability to bind BiP in stable transgenic overexpression lines. BiP bound normally to myc-bZIP28Δ591 but did not coimmunoprecipitate with myc-bZIP28Δ355, the construct lacking most of the C-terminal tail (Figure 3B). We also examined the localization and movement of YFP-tagged versions of the two truncation constructs. YFP-bZIP28Δ591 was retained in the ER under unstressed conditions and migrated to the nucleus only when seedlings were subjected to TM stress (Figures 3C and 3D). However, YFP-bZIP28Δ355 was located in the nucleus even under unstressed conditions (Figure 4A) and also under TM stressed conditions (Figure 4B). To demonstrate that YFP-bZIP28Δ355 is transcriptionally active in unstressed cells, we looked for the expression of a bZIP28 target gene, *BiP3* (Liu et al., 2007b). We found that unstressed seedlings expressing the full-length form of YFP-bZIP28 did not upregulate *BiP3*, but seedlings expressing YFP-bZIP28Δ355 upregulated *Bip3* expression even under unstressed conditions (see Supplemental Figure 6 online). Thus, bZIP28Δ355 does not bind to BiP and is not retained in the ER, but instead migrates to the nucleus in unstressed seedlings where it upregulates stress response genes.

It is possible that the YFP-bZIP28Δ355 truncation construct fails to be retained in the ER by shortcutting its normal route, which involves translocation through the secretion pathway to the Golgi where it would be released by S1P and S2P proteolysis. To test whether YFP-bZIP28Δ355 follows the conventional route to the nucleus, we introduced this construct into an *s2p* mutant background (Che et al., 2010). Under unstressed conditions, YFP-bZIP28Δ355 was prevented from moving constitutively into the nucleus (Figures 4C and 4D). In a wild-type background and under unstressed conditions, YFP-bZIP28Δ355 was observed not only in the nucleus, but also in small punctate structures that colocalize with a Golgi body marker (see Supplemental Figure 7 online). Thus, YFP-bZIP28Δ355 moved via the Golgi to the nucleus, and this was prevented by blocking proteolysis of the bZIP28 protein in an *s2p* mutant.

Identifying BiP Binding Regions in the C-Terminal Tail of bZIP28

Based on the results described above in which bZIP28Δ591 bound BiP and was retained in the ER under unstressed conditions, but bZIP28Δ355 did not bind BiP and was not retained in the ER, we focused on a region (positions 376 to 555) between these sites to identify the BiP binding and ER retention domains (Figure 3A). We initially attempted to use a yeast two-hybrid system to study the interaction between BiP and bZIP28. We had to abandon this approach due to high backgrounds in controls with the lumenal domain proteins. Blond-Elguindi et al. (1993) developed a means for identifying binding sites for mammalian BiP based on a phage-panning assay for octapeptides that bind to BiP. From their findings, they generated a scoring algorithm to identify potential BiP binding sites. However, their scoring algorithm did not allow us to unambiguously identify potential BiP binding sites in the lumenal tail of bZIP28. To better identify potential BiP binding sites in bZIP28, we conducted phage panning experiments using purified, immobilized *Arabidopsis* BiP1-His (see Supplemental Figure 8 online) and a phage library of 12 overlapping peptides (see Supplemental Table 1 online) from the lumenal domain of bZIP28 displayed in a M13 phage display system (Figure 5A).

We subjected the overlapping peptide phage library to four rounds of panning. Among the 25 phages sequenced from the second round of panning, we recovered eight of the 12 input

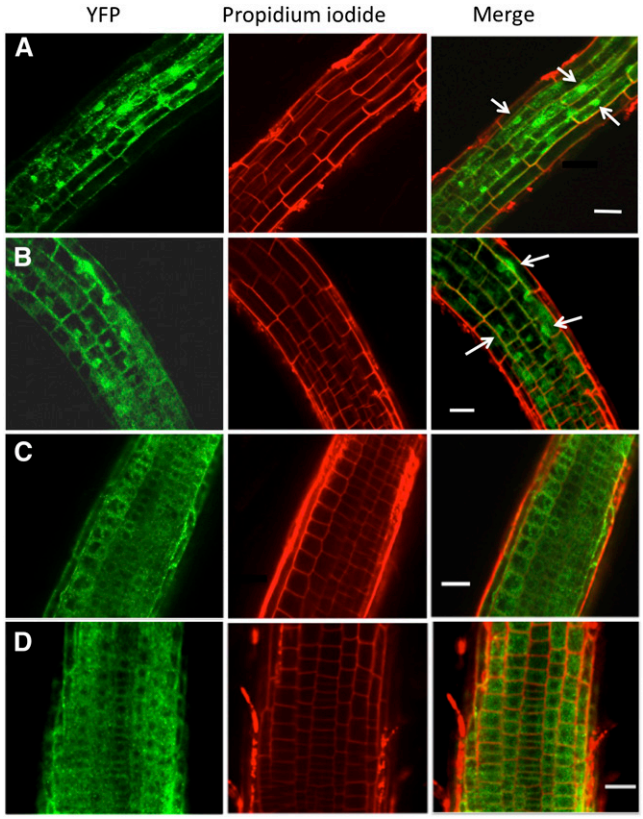

Figure 4. Translocation of bZIP28Δ355 to the Nucleus Requires S2P.

YFP-bZIP28Δ355 was imaged by confocal microscopy in a wild-type background at zero time **(A)** and after 1 h treatment **(B)** with 2 μg/mL TM. Arrows point out the nuclear localization of some of the YFP-bZIP28Δ355. YFP-bZIP28Δ355 was imaged in an *s2p* background at zero time **(C)** and after 1 h treatment **(D)** with TM. In each case the root cells were counterstained with propidium iodide. Bars = 50 μm.

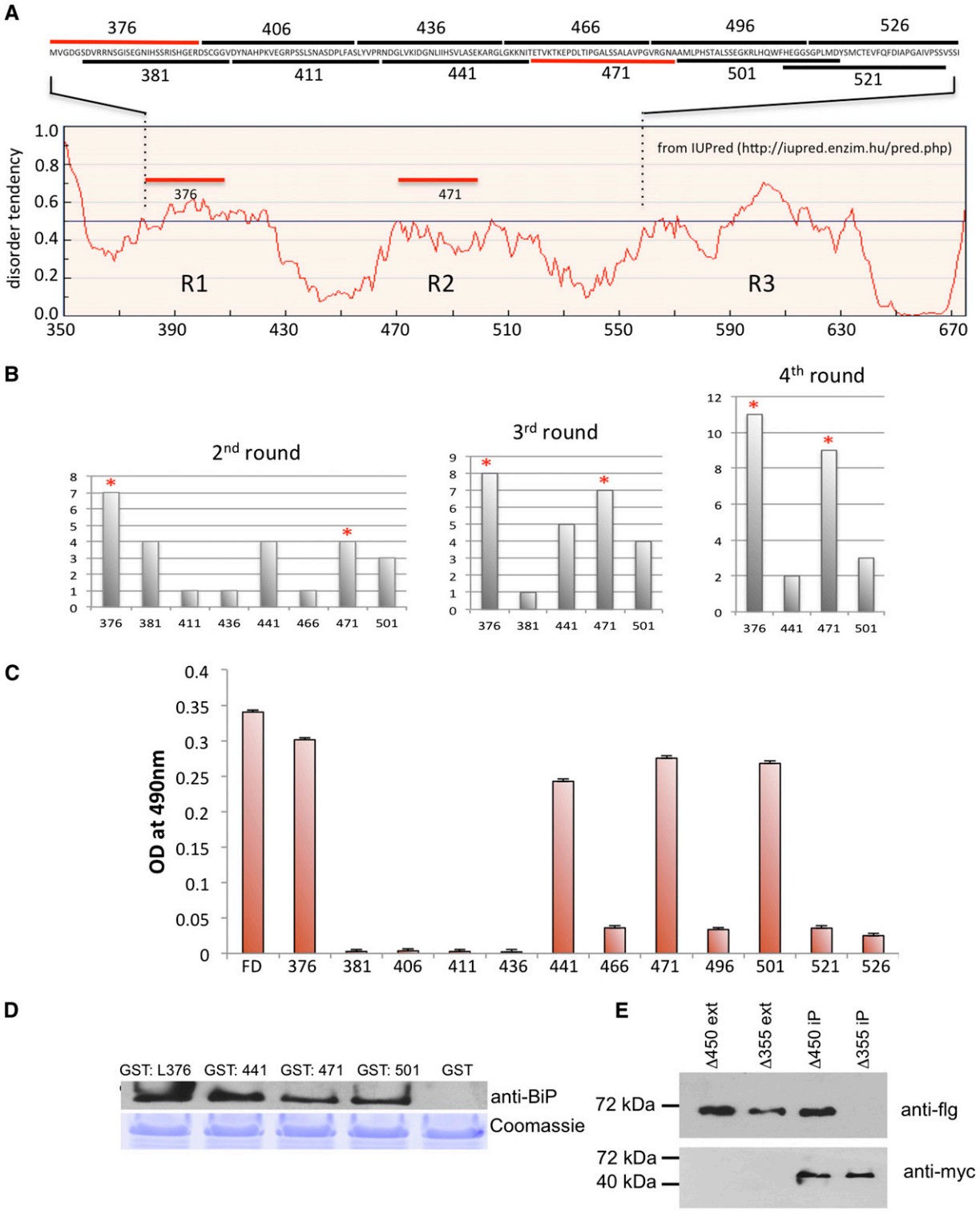

Figure 5. bZIP28 Peptides Used in Phage Display Library.

(A) Overlapping peptides from residues 376 to 555 in the lumenal domain of bZIP28 were displayed in M13 phage. Tendency for intrinsic disorder in the lumenal domain of bZIP28 is plotted against the map of the lumenal domain for bZIP28. The tendency for disorder was determined by IUPred (http://iupred.enzim.hu/pred.php).

sequences, and the phage displaying peptide 376 led all others in frequency of recovery (Figure 5B). In the third and fourth rounds, we recovered fewer sequences, but the recovered phage were enriched further for peptides 376 and 471. Thus, in the panning assay, peptides 376 and 471 clearly outcompeted the others in binding to immobilized BiP1. The results of the panning were confirmed by scoring the binding of phage separately to immobilized BiP1 in an ELISA assay (Figure 5C). When the peptides were not challenged competitively, the difference in the binding of phage displaying peptides 376 and 471 compared with phage-displaying peptides 441 and 501 was more modest. Nonetheless, the binding of these peptides to immobilized BiP1 was comparable to the binding of phage displaying the entire region covered by the peptide library. Also, to demonstrate that the binding of the peptides to immobilized BiP is not a contextual artifact, we performed protein overlay assays. The four peptides, 376, 441, 471, and 501, were fused to a glutathione *S*-transferase (GST) tag in a pET42a vector and expressed in BL-21 cells. The GST-tagged peptides were pulled down using glutathione beads and loaded on SDS gels. The blots were probed with purified BiP1-His followed by primary and secondary antibodies to detect the binding of BiP1 to the individual peptides. The four GST-tagged peptides were capable of binding to BiP1 (Figure 5D). The GST control and peptides that failed to bind to immobilized BiP in the panning procedures did not show any binding in the overlay assays (see Supplemental Figure 9 online).

In surveying the region covered by the phage panning analysis, it was observed that the peptides that showed the greatest binding to BiP were derived from regions of the bZIP28 lumenal tail that had the highest tendency for disorder (Figure 5A). In general, the bZIP28 C-terminal tail has three broad regions, labeled R1 to R3, that showed greater tendency for disorder. The tendency for disorder was determined by IUPred (http://iupred.enzim.hu/pred.php), a prediction program for disorder tendency based on the estimation of stabilizing contacts in the pairwise interactions between residues. Regions with fewer inter-residue interactions are predicted to be intrinsically unfolded regions (Dosztányi et al., 2005). The bZIP28 tail peptides that showed the greatest binding affinity for BiP1 were located in R1 and R2. These regions of bZIP28 showed little correlation with hydrophobicity index (see Supplemental Figure 10 online). It has been reported that BiP tends to bind to solvent-accessible hydrophobic patches on proteins (Caramelo et al., 2003). That does not appear to be case in the binding of BiP to the lumenal tail of bZIP28.

To determine if bZIP28 bearing the R1 region alone at its C-terminal tail could bind BiP, we developed another bZIP28 truncated construct, myc-bZIP28Δ450 (Figure 3A). This construct, along with BiP1-flg, was coexpressed in a tobacco leaf transient expression assay, and it was found that BiP1-flg coimmunoprecipitated with myc-bZIP28Δ450 in the leaf extracts (Figure 5E). We concluded that myc-bZIP28 bearing only the R1 region, which shows tendencies for disorder, can interact with BiP in planta. These results also demonstrated that BiP interacts independently with the different regions of the bZIP28 lumen-facing tail.

Effect of Overexpression of BiP on the Mobilization of bZIP28

We manipulated the levels of *BiP* expression to explore its impact on bZIP28 mobilization. *Arabidopsis* has three *BiP* genes, but since *BiP1* and *BiP2* are nearly identical, we overexpressed *BiP1* and *BiP3* with the 35S promoter in lines containing YFP-bZIP28 (see Supplemental Figure 11 online). To demonstrate that the overexpressed forms are appropriately localized at the subcellular level, we showed that BiP1-YFP-HDEL colocalized with an ER marker, sPMcherry (see Supplemental Figure 12 online). In the wild-type lines (not containing the *BiP1* or *BiP3* transgenes), YFP-bZIP28 was located in the ER in unstressed seedlings (Figure 6A) and translocated to nuclei after 2 h of TM treatment (Figure 6B). However, in *BiP1* and *BiP3* overexpressors, most YFP-bZIP28 was retained in the ER even after 2 h of TM treatment (Figures 6C and 6D). Although *BiP1* and *BiP3* were overexpressed, TM treatment still induced ER stress as evidenced by the splicing of bZIP60 (see Supplemental Figure 13 online and Deng et al., 2011). Nonetheless, *BiP1* or *BiP3* overexpression interfered with the release of YFP-bZIP28 from the ER. As a control, we showed that overexpression of BiP1P503L-flg, the construct that is defective in substrate binding, did not prevent bZIP28's movement to nuclei following stress treatment (Figure 6E).

To determine if we could further restrain the stress mobilization of YFP-bZIP28 by preventing its dissociation from BiP, we introduced into *Arabidopsis* mutated forms of BiP (BiPG235D) that are known in other systems to interfere with ATP binding and the release of client proteins (Wei and Hendershot, 1995;

Figure 5. (continued).

(B) Recombinant phages were pooled and panned against immobilized BiP1-His in four rounds of panning. At each round, bound phages were released and the inserts encoding the bZIP28 peptides were sequenced. The frequency in recovering phage expressing the various peptides in progressive rounds of screening is shown. Red asterisks indicate the peptides in phage recovered with the highest frequency in the fourth round of panning.

(C) Separate recombinant phage lines were incubated with immobilized BiP1-His, and bound phage were quantified in an ELISA assay. Error bars indicate SE.

(D) Overlay immunoblot demonstrating that soluble BiP1-His binds to GST-tagged bZIP28 peptides. The four peptides (441, 471, 376, and 501) enriched in panning were tagged with GST, purified by binding to glutathione beads, eluted, subjected to SDS-PAGE, and transferred to a nitrocellulose filter. The filter was incubated with purified BiP1-His, washed, and incubated with a primary anti-BiP antibody and then a secondary antibody was used to detect BiP binding. The GST-tagged peptides pulled down with glutathione beads and stained with Coomassie blue were used as a loading control.

(E) bZIP28 construct containing only the R1 region of lumenal domain (as shown in **[A]**) binds BiP1-flg in vivo. bZIP28 truncation constructs myc-bZIP28Δ450 (containing region R1) and myc-bZIP28Δ355 (lacking region R1) were each coexpressed with BiP1-flg in a tobacco leaf transient expression assay. Leaf extracts were subjected to immunoblotting and probed with anti-flg and anti-myc antibodies.

[See online article for color version of this figure.]

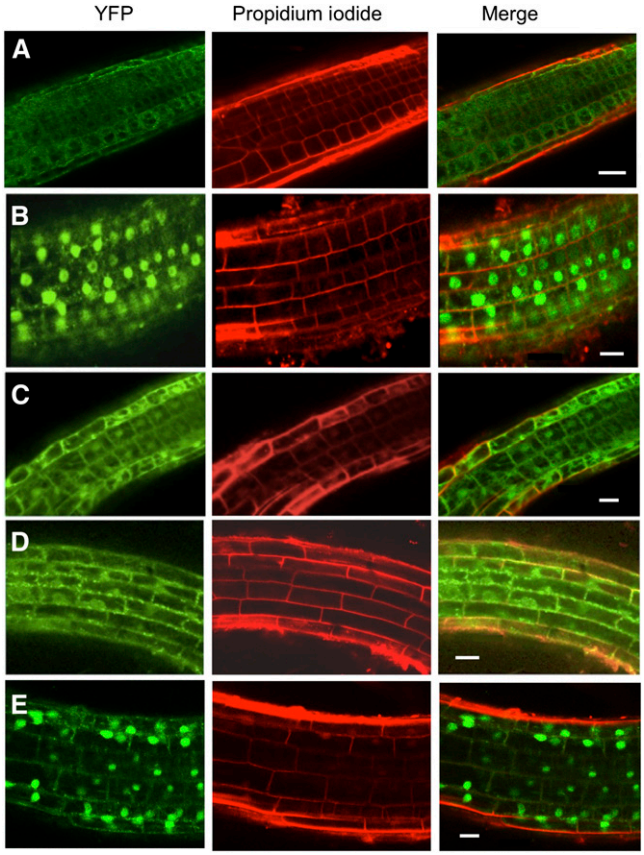

Figure 6. The Mobilization of bZIP28 in Lines Overexpressing BiP.

(A) YFP-bZIP28 localization in untreated *Arabidopsis* seedlings in a wild-type background.
(B) YFP-bZIP28 localization in wild-type *Arabidopsis* seedlings lines treated with 2 μg/mL TM for 2 h.
(C) YFP-bZIP28 localization in a line overexpressing *BiP1* from a 35Spromoter:BiP transgene treated with 2 μg/mL TM for 2 h.
(D) YFP-bZIP28 localization in lines overexpressing *BiP3* treated with 2 μg/mL TM for 2 h.
(E) YFP-bZIP28 localization in lines overexpressing BiP1P503L-flg (a form of BiP1 with a defect in substrate binding as shown in Figure 1D) treated with 2 μg/mL TM for 2 h. YFP fluorescence was imaged by confocal microscopy in roots counterstained with propidium iodide. Bars = 50 μm.

Snowden et al., 2007). In response to TM-induced stress, the expression of BiP1G233D or BiP3G247D transgenes appeared to prevent the dissociation from myc-bZIP28 in pull-down experiments (Figure 7A). The overexpression of BiP1G233D with reduced capacity for client protein dissociation prevented the processing of myc-bZIP28 in response to DTT treatment (Figure 7B) and also effectively blocked the nuclear relocation of YFP-bZIP28 in response to TM-induced stress (Figures 7C and 7D). DTT and not TM was used as a stress agent in this experiment because TM treatment produces additional nonglycosylated forms of myc-bZIP28 that make the gel patterns difficult to interpret. In our hands, DTT has been just as effective as TM in eliciting ER stress. The overexpression BiP3G247D similarly prevented the relocation of YFP-bZIP28 to nuclei in response to TM-induced stress (Figure 7E). Thus, we conclude that overexpression of BiP, particularly forms of BiP that interfere with the release of client proteins, prevents the normal mobilization of bZIP28 from the ER to the nucleus by binding to bZIP28 and not allowing its release.

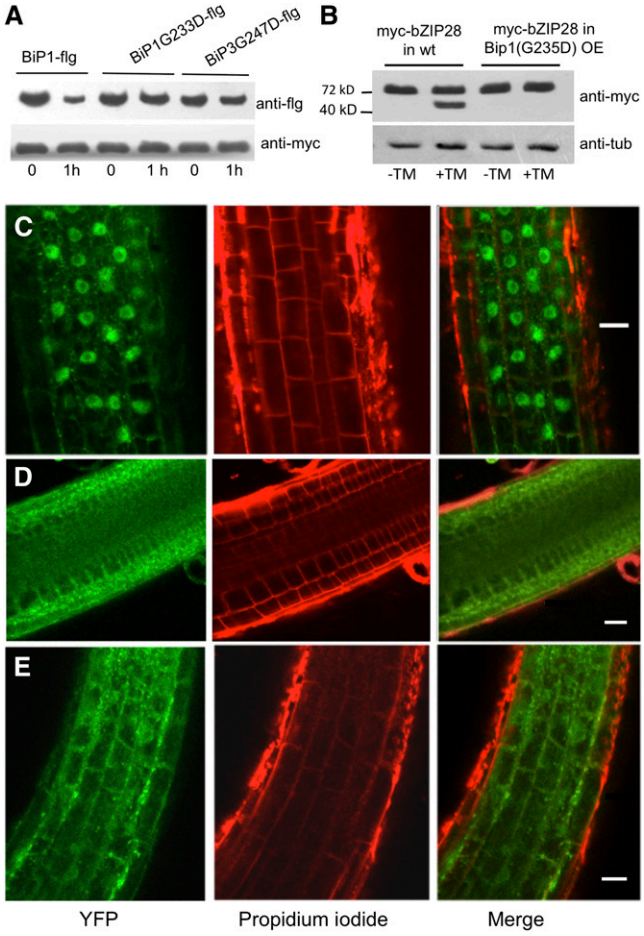

Figure 7. The Mobilization of bZIP28 in Lines Overexpressing Mutant Forms of BiP.

(A) Immunoprecipitation of myc-bZIP28 in extracts from *Arabidopsis* lines expressing flag-tagged mutated forms of BiP (BiP1G233D-flg and BipG247D-flg) that are predicted to be defective in binding ATP and releasing client proteins. Seedlings were treated with 2 μg/mL TM for 2 h to determine whether the BiP constructs dissociated from myc-bZIP28. Immunoblot of extracted proteins was probed with anti-flg and anti-myc.
(B) Processing of YFP-bZIP28 in wild-type (wt) and BiP1G233D-flg overexpressing (OE) backgrounds. Seedlings were either untreated or treated with 2 mM DTT for 2 h. Immunoblot of extracted proteins was probed with anti-myc and antitubulin as a loading control.
(C) YFP-bZIP28 localization in wild-type *Arabidopsis* seedlings lines treated with TM for 2 h.
(D) and **(E)** YFP-bZIP28 localization in lines overexpressing BiP1G233D **(D)** or BiP3G247D **(E)**, mutants with defects in ATP binding and release of client proteins. Lines were treated with TM for 2 h. YFP fluorescence was imaged by confocal microscopy in roots counterstained with propidium iodide. Bars = 50 μm.

Effect of BiP Knockouts on bZIP28 Mobilization

Similar experiments were conducted in BiP knockout lines containing YFP-bZIP28. Our interest here was whether the knockout of BiP genes would prevent the retention of bZIP28 in the ER under unstressed conditions. Homozygous T-DNA insertion lines are available for all three *BiP* genes; however, multiple mutants, such as the *bip1 bip2* double mutant, are not viable. In an effort to reduce BiP levels as much as possible, we obtained lines homozygous for either *bip1* or *bip2* but heterozygous for the other locus as described by Maruyama et al. (2010). The *BiP3* T-DNA homozygous insertion line (GK-075D06-011890) was obtained from the Nottingham Arabidopsis Stock Centre and found not to produce *BiP3* transcripts under stress conditions (see Supplemental Figure 14 online). Compared with the wild type, detectable amounts of YFP-bZIP28 escaped from the ER to nuclei under unstressed conditions in the *bip1*/*bip1 bip2*/+ and in the *bip1*/+ *bip2*/*bip2* and *bip3* mutant lines, indicating a reduced ability of the *BiP* knockout mutants to retain bZIP28 in the ER (Figures 8A to 8D). We observed processed myc-bZIP28 in the various knockout mutant lines under unstressed conditions, confirming these results and indicating that bZIP28 is constitutively activated in these lines (Figure 8E).

DISCUSSION

Our results show that BiP binds to bZIP28 under unstressed conditions and appears to bind to it in the same manner as it does to other client proteins, such as CPY*. We have also shown that BiP dissociates from bZIP28 in response to ER stress, and in doing so bZIP28 is activated, allowing it to make its way to the nucleus where it upregulates stress response genes (Figures 9A and 9B). The release of bZIP28 from BiP corresponds closely with its exit from the ER, but its release is not dependent on the trafficking of bZIP28 from organelle to organelle. In animal systems, it is thought that BiP binding retains ATF6 in the ER under nonstress conditions, putatively by blocking ATF6's GLSs, preventing it from being transported through the secretory pathway (Shen et al., 2002). There are different ideas as to how BiP relinquishes its hold on ATF6 under stress conditions (Parmar and Schröder, 2012). One idea, called the dynamic competition model, is that BiP is competed away from ATF6 by misfolded proteins in the ER (Harding et al., 2002; Kaufman et al., 2002; Kimata et al., 2003). In this model, BiP bound to ATF6 is thought to be in equilibrium with free BiP and BiP associated with misfolded proteins, and when unfolded proteins accumulate in the ER as a result of stress, the binding of BiP to ATF6 would be competed away. Our results in *Arabidopsis* support such a dynamic competition model.

We observed that the overexpression of BiP1 or BiP3 delays or blocks the translocation of YFP-bZIP28 to the nucleus. When BiP is overexpressed, bZIP28 appears not to be fully deployed in response to stress but seems to be largely retained in the ER. The overexpression effect is enhanced using mutant versions of BiP, which interfere with the release of substrates, as has also been shown by Snowden et al. (2007). On the other hand, overexpression of Bip1P503L defective in substrate binding does not block the movement of bZIP28. In animal systems, similar results were also observed by Shen et al. (2002), who overexpressed BiP in HeLa

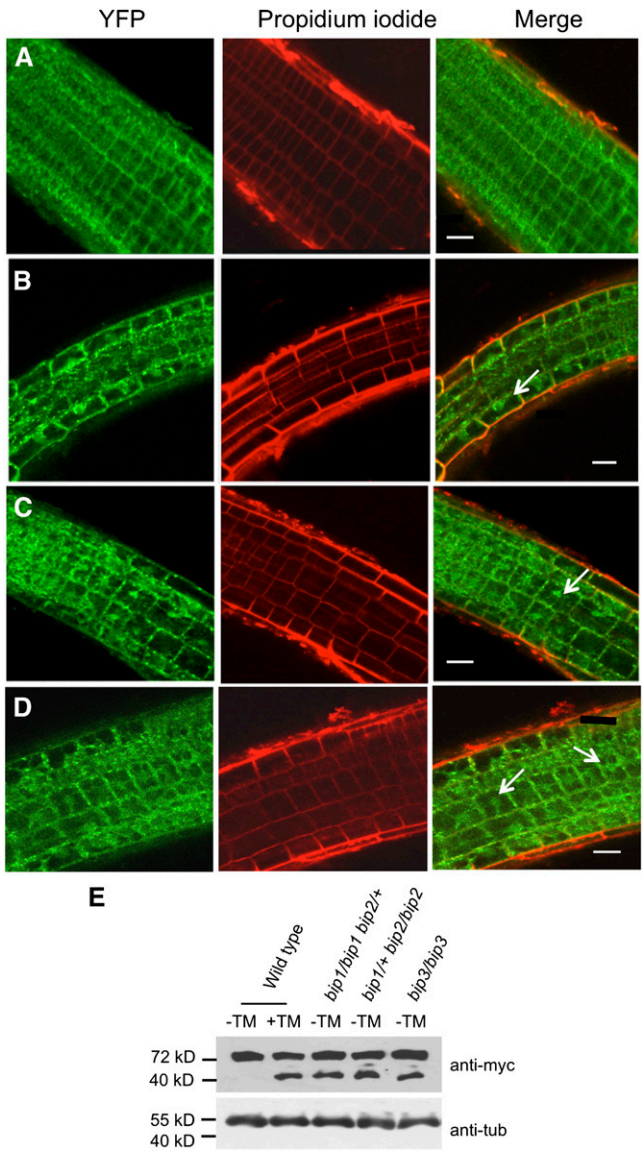

Figure 8. Mobilization of bZIP28 in *BiP* Knockout Lines.

(A) YFP-bZIP28 in wild-type unstressed *Arabidopsis* seedlings.
(B) to **(D)** YFP-bZIP28 in the *bip1*/*bip1 bip2*/+ **(B)**, *bip1*/+ *bip2*/*bip2* **(C)**, and *bip3*/*bip3* **(D)** mutant lines. YFP fluorescence was imaged by confocal microscopy in roots stained with propidium iodide. Arrows point out nuclear localization. Bars = 50 μm.
(E) Proteolytic processing of mycbZIP28 in wild-type seedlings in response to 2 μg/mL TM treatment for 2 h. Processing of myc-bZIP28 in untreated BiP knockout lines as indicated.

cells and found that ATF6 translocated to the Golgi, but processing by S1P and S2P, the Golgi resident proteases, was delayed following stress treatment. Also, overexpression of BiPT37G, an ATPase mutant compromised in the release of bound proteins, prevented the translocation of ATF6 to the Golgi and its processing by the Golgi-resident proteases (Wei et al., 1995). The BiP knockout mutants (*bip1*/*bip1 bip2*/+, *bip1*/+ *bip2*/*bip2*, and *bip3*/*bip3*) allow some migration of bZIP28 to nuclei under unstressed conditions.

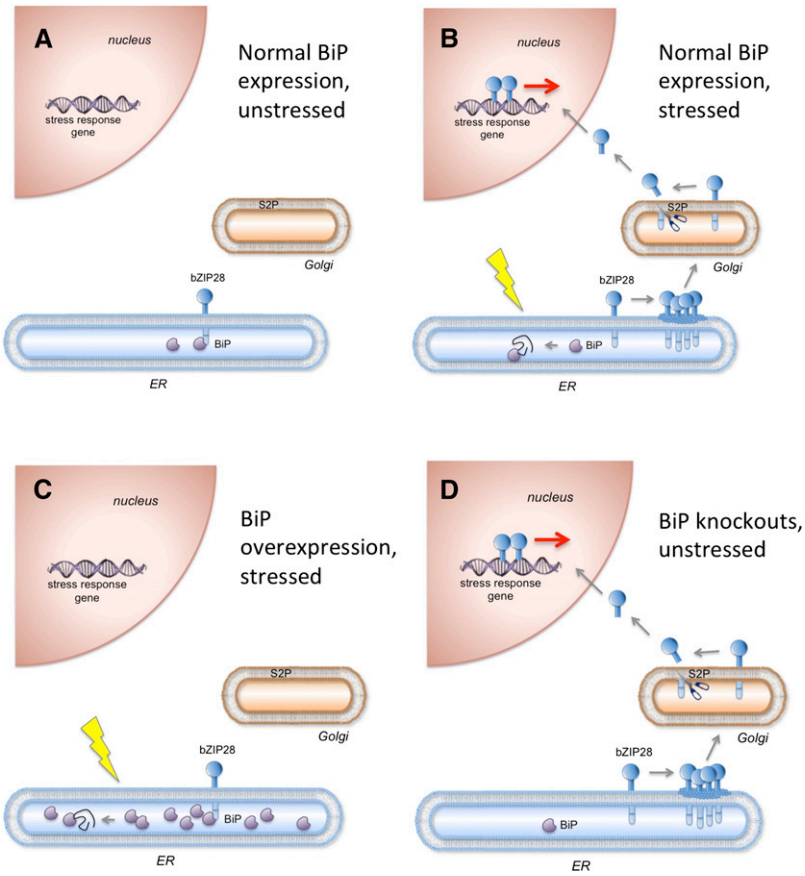

Figure 9. The Effect of BiP Expression on the Mobilization of bZIP28.

(A) BiP normally associates with bZIP28 under unstressed conditions and detains bZIP28 in the ER.
(B) In response to stress, BiP is competed away by the accumulation of misfolded proteins, releasing bZIP28 to relocate to the nucleus via the Golgi.
(C) When BiP is overexpressed, the accumulation of misfolded proteins fails to compete BiP away from bZIP28 under stress. As a result bZIP28 is detained in the ER even under stress conditions.
(D) When BiP is underexpressed, bZIP28 escapes to the nucleus under unstressed conditions.
[See online article for color version of this figure.]

All three *BiP* genes cannot be knocked out because even homozygous *bip1 bip2* mutants are not viable (Maruyama et al., 2010). We observed that these partial knockdown BiP mutants appear to be defective in retaining bZIP28 in the ER under unstressed conditions. In all, our results involving the overexpression and underexpression of BiP have demonstrated the critical role of BiP in the retention and activation of bZIP28 in *Arabidopsis*.

Another model for the release of ATF6 from BiP in animal systems does not invoke dynamic competition, instead positing that the association is stable, but can be disrupted by a signal from misfolded proteins. Several arguments favor a stability model (Shen et al., 2005), with one being that association between BiP and ATF6 is stable enough to survive immunoprecipitations without the need for cross-linking. Second, if BiP is continually binding and dissociating from ATF6, then the T37G BiP mutant with a defect in ATPase activity (protein releasing activity) should build up on ATF6 when introduced into monkey kidney fibroblast cells. Apparently, it does not (Shen et al., 2005). Shen et al. (2005) compared the dissociation of BiP from ATF6 and from unassembled Ig heavy chains, which are also retained in the ER by their association with BiP. They found that in response to stress, BiP dissociated from ATF6, but not from unassembled Ig heavy chains. From this they hypothesized that ATF6 contains BiP binding and release elements, the latter referred to as stress-responsive domains.

Our experiments demonstrate that BiP binds to the C-terminal, lumen-facing tail of bZIP28, and when the tail is eliminated as in bZIP28Δ355, the protein is not retained in the ER and behaves like an activated form of bZIP28. Truncated bZIP28 constitutively moves to the nucleus where it upregulates stress genes, including *BiP3*. The movement takes place via the Golgi and requires S2P processing. As an aside, it is interesting that YFP-bZIP28Δ355 appears to require S2P to relocate to the nucleus and is apparently a substrate for S2P. YFP-bZIP28Δ355 lacks most of its C-terminal tail and its S1P site. Cleavage at the S1P site is usually considered to be a prerequisite for S2P cleavage (Espenshade et al., 1999; Shen and Prywes, 2004). The implication from this is that S1P cleavage is not required for S2P proteolysis as long as the C-terminal tail on bZIP28 has been removed.

BiP is a chaperone that binds to nascent and misfolded proteins. So why does BiP bind to the lumen-facing tail of bZIP28? Our findings suggest that BiP binds to intrinsically disordered regions of the bZIP28 tail, regions that may have the properties of unfolded proteins. There are three regions in bZIP28's C-terminal tail that are predicted to be more disordered based on the algorithm at IUPRED (http://iupred.enzim.hu/pred.php), and peptides from two of these regions, R1 and R2, bind to BiP1 more avidly. The amino acid sequence in R1 is not conserved among various plant species; however, the pattern for disorder in that region is conserved among several species. It should be pointed out, nonetheless, that there is not much support in the literature for chaperones to bind to intrinsically disordered proteins; in fact, one meta-analysis of interactomes shows a negative correlation between the interactions between chaperones and intrinsically disordered proteins (Hegyi and Tompa, 2008).

Foresti et al. (2003) identified regions of bean (*Phaseolus vulgaris*) phaseolin that bound to BiP in plant cells. Earlier studies had shown that phaseolin mutants lacking the C-terminal domain failed to assemble into trimers (Pedrazzini et al., 1994, 1997; Frigerio et al., 2001). Based on the supposition that BiP binding increases the efficiency of the folding and assembly of secretory proteins, they searched for BiP binding sites in the C-terminal domain. To look for BiP binding sites, they appended the C-terminal domain containing three α-helical segments onto GFP and showed that the domain was sufficient to bind BiP. Foresti et al. (2003) attributed the binding to the hydrophobicity of the C-terminal domain. However, C-terminal domain of phaseolin is not more hydrophobic than several other regions of the protein. The C terminus is predicted to be somewhat more disordered than the rest of the protein, but the subterminal region to which BiP also binds is not particularly disordered. It is possible that preferred BiP binding sites might depend on other properties in addition to the tendency for disorder. Those properties need further definition because existing algorithms are not sufficiently predictive to identify BiP binding sites (Blond-Elguindi et al., 1993).

To sum up, our experiments demonstrate that the BiPs in *Arabidopsis* are master regulators of the membrane-associated transcription factor arm of the UPR signaling pathway in response to stress and function by binding to the intrinsically disordered regions of the C-terminal tail of bZIP28.

METHODS

Plant Material and Stress Treatments

Arabidopsis thaliana ecotype Columbia-0 was used in this study. Seeds were stratified at 4°C for 3 d prior to germination. Plants were grown under continuous white light at 23 to 25°C in soil or on Linsmaier/Skoog (LS) medium (1× LS salts, 1% Suc, and 0.8% agar). *Agrobacterium tumefaciens*–mediated transformation was performed using the floral dip method (Bechtold et al., 1993). *Agrobacterium* strain GV3101 was used in all transformation experiments. For stress treatment, 7-d-old seedlings were treated with 2 μg mL^{-1} TM or 2 mM DTT in LS medium for the times indicated.

For confocal microscopy, single and double transgenic plants were generated by successive floral dips of constructs. The double transgenics involving mCherry-tagged CDC markers were as follows: 35S:YFP-bZIP28 with the Golgi marker CDC-968 or with the ER marker CDC-960, and 35S:Bip1-YFP-HDEL with spMcherry, 35S:YFPΔ355 with the Golgi marker CDC-968, 35S:Bip1-flg-HDEL with myc-28, 35S:B1P3-flg-HDEL with myc-28; 35S:Bip1G233D-flg-HDEL with myc-28; 35S:Bip1-HDEL-S with YFP-bZIP28 and 35S:B1P3-HDEL-S with YFP-bZIP28. Single transgenic lines were generated for YFP-bZIP28Δ591, YFP-bZIP28Δ355, myc-bZIP28Δ591,myc-bZIP28Δ355, and CPY*-GFP. The ER marker CDC-960 and Golgi marker CDC-968 were obtained from the ABRC.

T-DNA mutant line with an insertion in the first exon of *BiP3* (GK-075D06-011890) was obtained from the Nottingham Arabidopsis Stock Centre (N744092). The T-DNA lines were genotyped by PCR using gene-specific primers and a left border T-DNA primer (see Supplemental Table 2 online). The insertion lines were further treated with TM for 30 min to affirm the loss of BiP3 transcripts. The *bip1* and *bip2* mutant lines were kindly provided by the Shuh-ichi Nishikawa Lab (Nagoya University). The lines were described by Maruyama et al. (2010). Since the double homozygous lines are female sterile, they are maintained as *bip1*/+ *bip2*/*bip2* or *bip1*/*bip1* *bip2*/+ strains. The *s2p* mutant line was described by Che et al., (2010) and was kindly provided by Ping Che (DuPont Pioneer Hi-Bred International).

Plasmid Construction

Plasmid constructs were prepared as summarized in Supplemental Table 3 online using the primers listed in Supplemental Table 2 online.

The open reading frame of bZIP28 (At3g10800) was amplified from 1-week-old seedlings by RT-PCR using primer pair Zip28 (see Supplemental Table 2 online). The product was cloned into pSKM36 (Liu et al., 2007b) at the *Asc*I and *Spe*I sites, resulting in pMZIP28, which was used as a template for further constructs. pMZip28 was tagged with monomeric GFP by amplifying it from a GFP vector using GFPAsc primers and inserting it into the *Asc*I site to generate N-terminal monomeric GFP–tagged bZIP28. A 4× epitope myc tag (EQKLISEEDLRN) was amplified from pSKM36 using the primer MycAsc (including the ATG before the myc sequence) and inserted into pMZIP28 at the *Asc*I site to generate N-terminal myc-tagged bZIP28. The construction of bZIP28KK311AA, bZIP28KK320AA, and bZIPG329A mutants has been described previously by Srivastava et al. (2012). The vectors pSKM36 and pSKY are described by Srivastava et al. (2012). The open reading frames of *BiP1* and *BiP3* were amplified from 10-d-old seedlings (for *Bip3*; cDNAs were generated from the RNA of seedlings treated for 30 min with TM) using the primers Bip1SKHDELStopPr and Bip3HDELStopPr listed in Supplemental Table 2 online. The templates were called Bip1SKHDELStop and Bip3HDELStop. The Flag and YFP tags with HDEL sequences (as required) were attached to the C terminus of BiP1 and BiP3 using the enzyme *Spe*I. The BiP1G233D and BiP3G247D mutations were prepared by overlapping PCR using the primers listed and the templates Bip1SKHDELStop and Bip3HDELStop. The signal peptide chitinase mCherry marker was prepared by amplifying the CSP-YFP-HDEL obtained from Edgar Cahoon (University of Nebraska) (Chen et al., 2008) using the primers spMcherry and ligated into the vector pCHF1 with HDEL sequence at its C terminus to retain the protein in the ER.

Cloning of the peptides from the C terminus of bZIP28 was performed in pCANTB SE at the *Sfi*I and *Not*I sites using pMZIP28 as template and the primers are listed in Supplemental Table 2 online. bZIP28 was cloned in pET28 at the *Bam*HI and *Not*I sites and expressed in BL-21 cells.

Transient Transformation in Tobacco

Transient expression in tobacco (*Nicotiana tabacum*) leaf epidermis was performed as described previously (Batoko et al., 2000) using *Agrobacterium* (OD_{600} = 0.05) containing the binary vectors pSKY and pSKM36.

Immunoprecipitations

To prepare plant extracts for immunoprecipitations of myc-tagged proteins, 5 g of seedlings was ground in liquid nitrogen and suspended in 25 mM Tris/HCl, pH 7.2, 150 mm NaCl, 0.1% Nonidet P-40 (Calbiochem),

and 10% glycerol. Anti-c-myc agarose conjugate (Sigma-Aldrich) was added to the filtered lysate and incubated for 2 h at 4°C. The mixture was rotated at 4°C for 2 h, and beads were washed four times for 5 min each with the buffer described above. The recovered beads were resuspended and boiled in 2× SDS buffer for 5 min, and the eluted material was subjected to immunoblotting. Plant crude extracts (input material for the immunoprecipitation reactions) were analyzed for the presence of the tagged protein using c-myc antibody (9E10; Santa Cruz Biotechnology) as probe. BiP-bound proteins were immunoprecipitated from 2 g of plant material using a BiP antibody, ADI-SPA-818 D from Enzo Life Sciences. The mixture was rotated at 4°C for 2 h. This was followed by binding to protein agarose 916-157 (Millipore), and bound beads were washed four times for 5 min each with the buffer described above followed by loading on SDS gel. Flag antibodies (F1804; Sigma-Aldrich) and GFP antibodies (11814460001; Roche) were used in immunoprecipitations and in probing immunoblots.

Immunoblot Analysis

Immunoblots were performed as described by Liu et al. (2007a, 2007b). To examine the processing of bZIP28, plants were grown vertically on Petri plates containing agar medium. Ten-day-old seedlings were treated with 2 mm DTT in LS medium, and 300 mg of root material was harvested from the treated plants. Roots were homogenized in liquid nitrogen, and 30 μg of protein was loaded per lane on gels. T8203 monoclonal anti-αtubulin antibody from Sigma-Aldrich was used to detect tubulin as a loading control.

Confocal Microscopy

Subcellular localization and protein movement experiments for fluorescent-tagged proteins were performed using a NikonC1si confocal scanning system attached to a 90i microscope (Nikon Instruments). Roots were used for microscopy from plants pretreated with TM, and untreated plants were used as controls. The roots were observed under ×20 and ×60 water lenses. Some roots were counterstained with 50 mg mL^{-1} propidium iodide and Syto Red. The emission signals for YFP, propidium iodide, and SYTO Red 59 were acquired using sequential scanning mode to eliminate crosstalk and emission signal bleed-through. Fluorescence emission was obtained by laser excitation of YFP at 488 nm, and for mCherry, propidium iodide, or Syto Red, excitation was at 591 nm. Emission was in the range 500 to 575 and 590 to 700 nm, respectively. Syto Red 59 (S-11341) was obtained from Molecular Probes.

Gene Expression Analysis

Total RNA was isolated from ground plant tissues using an RNeasy kit, treated with RNase-free DNase I, according to the manufacturer's instructions (Qiagen), and was quantified by 260/280-nm UV light absorption. A 1-μg portion of total RNA was reverse transcribed using the Supertranscript III RT kit (Invitrogen). A 2-μL volume of cDNA was used for RT-PCR. All primers are listed in Supplemental Table 2 online.

Construction of Phage-Displayed Overlapping Peptide Library

Twelve overlapping regions of the lumenal domain of bZIP28 were generated by PCR using bZIP28 cDNA as a template and forward and reverse primers to incorporate *Sfi*I and *Not*I sites. The PCR fragments were then digested with *Sfi*I and *Not*I, ligated into a similarly digested pCANTAB 5E phagemid vector, and subsequently transformed into *Escherichia coli* XL1-Blue cells (Stratagene). Single colonies from each plate were inoculated into 5 mL 2YT/carbenicillin/tetracycline media, grown to OD_{600} of ~0.2 to 0.3 at 37°C and then infected with helper phage-VCSM13 (Stratagene). After 1 h, the cell culture was transferred to 25 mL 2YT/Kan media and further incubated overnight at 37°C. After removing cell debris by centrifugation, phage particles were precipitated from the supernatant using 7.5 mL 20% polyethylene glycol solution containing 2.5 M NaCl. The precipitate was resuspended in 1 mL PBS, and the phage concentration was determined by measuring absorbance at 268 λ (OD_{268} = 1.0 for a solution containing 5×10^{12} phage per mL). A peptide library was prepared by mixing equal concentrations of individual phage peptide.

Production and Purification of BiP for Phage Panning Experiment

BiP1 was His tagged at its N terminus in the pET28a vector. The construct was introduced into *E. coli* strain BL21, and cells were induced with 300 μM isopropyl β-D-1 thiogalacopyranodise overnight at 16°C. His-tagged BiP1 was purified using nickel-nitrilotriacetic acid agarose beads (Qiagen). The incubation buffer contained 50 mM sodium phosphate buffer, pH 8.0, 300 mM NaCl, 20 mM imidazole, and 0.05% Tween. The mixture was rotated at 4°C for 2 h and washed four times with incubation buffer. The protein was eluted by increasing the imidazole concentration in the incubation buffer to 250 mM. The beads were resuspended and boiled in 2× SDS buffer for 5 min and subjected to SDS-PAGE to check for purity. The purified BiP-His was used for panning experiments, ELISA, and overlay immunoblotting.

Phage Panning

His-tagged BiP1 protein was immobilized in the wells of a Nunc Maxisorp ELISA plate by aliquoting 100 μL of protein at a concentration of 10 μg/mL in 50 mM $NaHCO_3$, pH 9.6, at room temperature with gentle rotation for 2 h. Wells were then blocked with PBS containing 0.2% BSA for 1 h followed by three washings with PBS containing 0.05% Tween 20 (PBST) and then incubated with 100 μL of the phage peptide library from the lumenal domain of bZIP28 for 3 h at room temperature with gentle rotation. After removing unbound phage by washing with PBST five times, bound phage was eluted by incubating with 500 μL of 0.1 M HCl for 5 min at room temperature with shaking. The eluted phage were immediately neutralized by the addition of one-third phage volume of 1 M Tris-HCl buffer, pH 8.0, followed by infection of XL1-Blue cells (grown to <0.6 OD) with the phage. Infected XL1-Blue cells were incubated at 37°C for 20 min followed by addition of the helper phage (VCSM13) and again incubating at 37°C for 30 min. The phage-infected XL1-Blue cells were transferred into a conical flask containing 50 mL of 2YT medium containing 10 μg/mL of tetracycline and 100 μg/mL of ampicillin that was further incubated at 37°C overnight with shaking at 210 rpm. Phage was prepared as described earlier, yielding the first round of enriched phage. The entire process was repeated for four rounds, and after two, three, and four rounds, phage-infected XL1-Blue cells were grown on 2YT ampicillin plates. Plasmids were prepared from 25 randomly selected colonies and their DNA sequenced.

Phage ELISA for Binding Specificity

For phage ELISAs, 100 μL of His-tagged BiP1 protein and BSA (control) (10 μg/mL in 50 mM $NaHCO_3$, pH 9.6) were immobilized in the wells of an ELISA plate at room temperature with gentle rotation for 2 h. The plate was then washed two times with PBS followed by blocking with PBST containing 0.2% BSA for 1 h. Subsequently, after three washings with PBST, wells were incubated with the 100 μL of phage displaying lumenal domain peptides diluted in PBST containing 0.2% BSA for 2 h at room temperature with gentle shaking. The plate was again washed three times with PBST followed by incubation with anti-M13 HRP conjugated antibody for 1 h. After washing four more times with PBST, bound phage in each well was detected by incubating for ~10 min with 50 μL of a solution containing 0.01% hydrogen peroxide and 0.8 mg/mL *o*-phenylenediamine dihydrochoride. Reactions were terminated by the addition of 50 μL 3M HCl, and absorbance of the developed yellow color was measured at 490 nm.

Overlay Immunoblotting

The four peptides (441, 471, 376, and 501) were tagged on their N terminus with a GST tag in pET42a vector. For in vitro GST pull-down assays, GST-441, GST-471, GST-376, GST-501, and GST-H6 (control) were bound to glutathione agarose beads (Sigma-Aldrich). The pull-down mixture contained 25 mM Tris-HCl, pH 7.4, 75 mM NaCl, 0.5 mM EDTA, 0.5 mM DTT, 0.05% Nonidet P-40, and 1 mg/mL BSA (NEB). The mixture was rotated at 4°C for 2 h and washed four times with pull-down buffer. The beads were resuspended and boiled in 2× SDS buffer for 5 min, and the eluted material was subjected to SDS-PAGE. GST-tagged peptides were transferred onto a nitrocellulose membrane after separation on SDS-PAGE, and the membrane was blocked with 1% BSA in TBS buffer. Ten micrograms of BiP protein was allowed to bind to the respective peptides by incubation in T-TBS buffer containing 0.1% BSA. This was followed by incubation of the blot with the BiP antibody, which was detected by a secondary antibody, as described in the immunoblotting procedure.

Accession Numbers

Sequence data from this article can be found in the Arabidopsis Genome Initiative or GenBank/EMBL databases under the following accession numbers: BiP1 (At5g28540), BiP2 (At5g42020), BiP3 (At1g09080), bZIP17 (At2g40950), bZIP28 (At3g10800), Erdj3a (At3g08970), Erdj3b (At3g62600), and S2P (At4g20310).

Supplemental Data

The following materials are available in the online version of this article.

Supplemental Figure 1. Sequence Alignment of the Three BiP Proteins from *Arabidopsis*.

Supplemental Figure 2. Immunoprecipitation of myc-bZIP28 by Bead-Bound BiP Antibody.

Supplemental Figure 3. BiP Binds CPY*-GFP Expressed as a Transgene in *Arabidopsis* Seedlings.

Supplemental Figure 4. BiP Levels in Stressed *Arabidopsis* Seedlings.

Supplemental Figure 5. Subcellular Localization of YFP-bZIP28 in Stressed Seedlings.

Supplemental Figure 6. Constitutive Expression of *BiP3* in a Line That Fails Retain bZIP28 in the ER.

Supplemental Figure 7. Subcellular Localization of YFP-bZIP28Δ355 in Unstressed Seedlings.

Supplemental Figure 8. BiP1-His Extracted from *E. coli*.

Supplemental Figure 9. BiP Binding to Peptides Enriched in Phage Display Panning.

Supplemental Figure 10. Hydrophobicity Plot of the Lumenal Domain of bZIP28.

Supplemental Figure 11. Expression Levels of BiP in Untreated BiP-Overepressing Lines.

Supplemental Figure 12. Subcellular Localization of BiP1-YFP-HDEL.

Supplemental Figure 13. bZIP60 Splicing in BiP Overexpression Lines.

Supplemental Figure 14. Noninduction of *BiP3* in *bip3* Homozygous Mutant.

Supplemental Table 1. List of Peptides Used in the Phage Display Experiments.

Supplemental Table 2. Primers Used in This Study.

Supplemental Table 3. Cloning Information.

ACKNOWLEDGMENTS

This work was supported by the Iowa State University Plant Sciences Institute and by a National Science Foundation grant (IOS90917) to S.H.H. The *bip1/bip1 bip2/+* and *bip1/+ bip2/bip2* mutant lines were obtained from the Shuh-ichi Nishikawa Lab (Nagoya University, Nagoya, Japan). The s2p mutant line was provided generously by Ping Che (DuPont Pioneer Hi-Bred International, Johnston, IA).

AUTHOR CONTRIBUTIONS

R.S., Y.D., S.S., and S.H.H. conceived and designed the experiments. R.S. and S.S. performed the experiments. R.S., S.S., and A.G.R. analyzed the data. R.S. and S.H.H. wrote the article.

Received February 13, 2013; revised March 28, 2013; accepted April 10, 2013; published April 24, 2013.

REFERENCES

Alvim, F.C., Carolino, S.M., Cascardo, J.C., Nunes, C.C., Martinez, C.A., Otoni, W.C., and Fontes, E.P. (2001). Enhanced accumulation of BiP in transgenic plants confers tolerance to water stress. Plant Physiol. **126:** 1042–1054.

Anelli, T., and Sitia, R. (2008). Protein quality control in the early secretory pathway. EMBO J. **27:** 315–327.

Batoko, H., Zheng, H.Q., Hawes, C., and Moore, I. (2000). A rab1 GTPase is required for transport between the endoplasmic reticulum and golgi apparatus and for normal Golgi movement in plants. Plant Cell **12:** 2201–2218.

Bechtold, N., Ellis, J., and Pelletier, G. (1993). In planta *Agrobacterium*-mediated gene transfer by infiltration of adult *Arabidopsis thaliana* plants. C. R. Acad. Sci. Paris **316:** 1194–1199.

Bertolotti, A., Zhang, Y., Hendershot, L.M., Harding, H.P., and Ron, D. (2000). Dynamic interaction of BiP and ER stress transducers in the unfolded-protein response. Nat. Cell Biol. **2:** 326–332.

Blond-Elguindi, S., Cwirla, S.E., Dower, W.J., Lipshutz, R.J., Sprang, S.R., Sambrook, J.F., and Gething, M.J. (1993). Affinity panning of a library of peptides displayed on bacteriophages reveals the binding specificity of BiP. Cell **75:** 717–728.

Caramelo, J.J., Castro, O.A., Alonso, L.G., De Prat-Gay, G., and Parodi, A.J. (2003). UDP-Glc:glycoprotein glucosyltransferase recognizes structured and solvent accessible hydrophobic patches in molten globule-like folding intermediates. Proc. Natl. Acad. Sci. USA **100:** 86–91.

Che, P., Bussell, J.D., Zhou, W., Estavillo, G.M., Pogson, B.J., and Smith, S.M. (2010). Signaling from the endoplasmic reticulum activates brassinosteroid signaling and promotes acclimation to stress in *Arabidopsis*. Sci. Signal. **3:** ra69.

Chen, M., Markham, J.E., Dietrich, C.R., Jaworski, J.G., and Cahoon, E.B. (2008). Sphingolipid long-chain base hydroxylation is important for growth and regulation of sphingolipid content and composition in *Arabidopsis*. Plant Cell **20:** 1862–1878.

Deng, Y., Humbert, S., Liu, J.X., Srivastava, R., Rothstein, S.J., and Howell, S.H. (2011). Heat induces the splicing by IRE1 of a mRNA encoding a transcription factor involved in the unfolded protein response in *Arabidopsis*. Proc. Natl. Acad. Sci. USA **108:** 7247–7252.

Dosztányi, Z., Csizmok, V., Tompa, P., and Simon, I. (2005). IUPred: Web server for the prediction of intrinsically unstructured regions of proteins based on estimated energy content. Bioinformatics **21:** 3433–3434.

Espenshade, P.J., Cheng, D., Goldstein, J.L., and Brown, M.S. (1999). Autocatalytic processing of site-1 protease removes propeptide and permits cleavage of sterol regulatory element-binding proteins. J. Biol. Chem. **274:** 22795–22804.

Foresti, O., Frigerio, L., Holkeri, H., de Virgilio, M., Vavassori, S., and Vitale, A. (2003). A phaseolin domain involved directly in trimer assembly is a determinant for binding by the chaperone BiP. Plant Cell **15:** 2464–2475.

Frigerio, L., Pastres, A., Prada, A., and Vitale, A. (2001). Influence of KDEL on the fate of trimeric or assembly-defective phaseolin: Selective use of an alternative route to vacuoles. Plant Cell **13:** 1109–1126.

Harding, H.P., Calfon, M., Urano, F., Novoa, I., and Ron, D. (2002). Transcriptional and translational control in the mammalian unfolded protein response. Annu. Rev. Cell Dev. Biol. **18:** 575–599.

Hegyi, H., and Tompa, P. (2008). Intrinsically disordered proteins display no preference for chaperone binding in vivo. PLoS Comput. Biol. **4:** e1000017.

Hendershot, L.M. (2004). The ER function BiP is a master regulator of ER function. Mt. Sinai J. Med. **71:** 289–297.

Iwata, Y., Fedoroff, N.V., and Koizumi, N. (2008). *Arabidopsis* bZIP60 is a proteolysis-activated transcription factor involved in the endoplasmic reticulum stress response. Plant Cell **20:** 3107–3121.

Iwata, Y., and Koizumi, N. (2005). An *Arabidopsis* transcription factor, AtbZIP60, regulates the endoplasmic reticulum stress response in a manner unique to plants. Proc. Natl. Acad. Sci. USA **102:** 5280–5285.

Iwata, Y., Sakiyama, M., Lee, M.-H., and Koizumi, N. (2010). Transcriptomic response of *Arabidopsis thaliana* to tunicamycin induced endoplasmic reticulum stress. Plant Biotechnol. **27:** 161–171.

Izawa, T., Nagai, H., Endo, T., and Nishikawa, S. (2012). Yos9p and Hrd1p mediate ER retention of misfolded proteins for ER-associated degradation. Mol. Biol. Cell **23:** 1283–1293.

Jin, Y., Awad, W., Petrova, K., and Hendershot, L.M. (2008). Regulated release of ERdj3 from unfolded proteins by BiP. EMBO J. **27:** 2873–2882.

Kaufman, R.J., Scheuner, D., Schröder, M., Shen, X., Lee, K., Liu, C.Y., and Arnold, S.M. (2002). The unfolded protein response in nutrient sensing and differentiation. Nat. Rev. Mol. Cell Biol. **3:** 411–421.

Kimata, Y., Kimata, Y.I., Shimizu, Y., Abe, H., Farcasanu, I.C., Takeuchi, M., Rose, M.D., and Kohno, K. (2003). Genetic evidence for a role of BiP/Kar2 that regulates Ire1 in response to accumulation of unfolded proteins. Mol. Biol. Cell **14:** 2559–2569.

Koizumi, N. (1996). Isolation and responses to stress of a gene that encodes a luminal binding protein in *Arabidopsis thaliana*. Plant Cell Physiol. **37:** 862–865.

Leborgne-Castel, N., Jelitto-Van Dooren, E.P., Crofts, A.J., and Denecke, J. (1999). Overexpression of BiP in tobacco alleviates endoplasmic reticulum stress. Plant Cell **11:** 459–470.

Liu, J.X., and Howell, S.H. (2010). bZIP28 and NF-Y transcription factors are activated by ER stress and assemble into a transcriptional complex to regulate stress response genes in *Arabidopsis*. Plant Cell **22:** 782–796.

Liu, J.X., Srivastava, R., Che, P., and Howell, S.H. (2007a). Salt stress responses in *Arabidopsis* utilize a signal transduction pathway related to endoplasmic reticulum stress signaling. Plant J. **51:** 897–909.

Liu, J.X., Srivastava, R., Che, P., and Howell, S.H. (2007b). An endoplasmic reticulum stress response in *Arabidopsis* is mediated by proteolytic processing and nuclear relocation of a membrane-associated transcription factor, bZIP28. Plant Cell **19:** 4111–4119.

Martínez, I.M., and Chrispeels, M.J. (2003). Genomic analysis of the unfolded protein response in *Arabidopsis* shows its connection to important cellular processes. Plant Cell **15:** 561–576.

Maruyama, D., Endo, T., and Nishikawa, S. (2010). BiP-mediated polar nuclei fusion is essential for the regulation of endosperm nuclei proliferation in *Arabidopsis thaliana*. Proc. Natl. Acad. Sci. USA **107:** 1684–1689.

Nekrasov, V., et al. (2009). Control of the pattern-recognition receptor EFR by an ER protein complex in plant immunity. EMBO J. **28:** 3428–3438.

Otero, J.H., Lizák, B., and Hendershot, L.M. (2010). Life and death of a BiP substrate. Semin. Cell Dev. Biol. **21:** 472–478.

Parmar, V.M., and Schröder, M. (2012). Sensing endoplasmic reticulum stress. Adv. Exp. Med. Biol. **738:** 153–168.

Pedrazzini, E., Giovinazzo, G., Bollini, R., Ceriotti, A., and Vitale, A. (1994). Binding of BiP to an assembly-defective protein in plant cells. Plant J. **5:** 103–110.

Pedrazzini, E., Giovinazzo, G., Bielli, A., de Virgilio, M., Frigerio, L., Pesca, M., Faoro, F., Bollini, R., Ceriotti, A., and Vitale, A. (1997). Protein quality control along the route to the plant vacuole. Plant Cell **9:** 1869–1880.

Reis, P.A., Rosado, G.L., Silva, L.A., Oliveira, L.C., Oliveira, L.B., Costa, M.D., Alvim, F.C., and Fontes, E.P. (2011). The binding protein BiP attenuates stress-induced cell death in soybean via modulation of the N-rich protein-mediated signaling pathway. Plant Physiol. **157:** 1853–1865.

Schott, A., Ravaud, S., Keller, S., Radzimanowski, J., Viotti, C., Hillmer, S., Sinning, I., and Strahl, S. (2010). *Arabidopsis* stromal-derived Factor2 (SDF2) is a crucial target of the unfolded protein response in the endoplasmic reticulum. J. Biol. Chem. **285:** 18113–18121.

Shen, J., Chen, X., Hendershot, L., and Prywes, R. (2002). ER stress regulation of ATF6 localization by dissociation of BiP/GRP78 binding and unmasking of Golgi localization signals. Dev. Cell **3:** 99–111.

Shen, J., and Prywes, R. (2004). Dependence of site-2 protease cleavage of ATF6 on prior site-1 protease digestion is determined by the size of the luminal domain of ATF6. J. Biol. Chem. **279:** 43046–43051.

Shen, J., Snapp, E.L., Lippincott-Schwartz, J., and Prywes, R. (2005). Stable binding of ATF6 to BiP in the endoplasmic reticulum stress response. Mol. Cell. Biol. **25:** 921–932.

Snowden, C.J., Leborgne-Castel, N., Wootton, L.J., Hadlington, J.L., and Denecke, J. (2007). In vivo analysis of the lumenal binding protein (BiP) reveals multiple functions of its ATPase domain. Plant J. **52:** 987–1000.

Srivastava, R., Chen, Y., Deng, Y., Brandizzi, F., and Howell, S.H. (2012). Elements proximal to and within the transmembrane domain mediate the organelle-to-organelle movement of bZIP28 under ER stress conditions. Plant J. **70:** 1033–1042.

Tajima, H., Iwata, Y., Iwano, M., Takayama, S., and Koizumi, N. (2008). Identification of an *Arabidopsis* transmembrane bZIP transcription factor involved in the endoplasmic reticulum stress response. Biochem. Biophys. Res. Commun. **374:** 242–247.

Valente, M.A., et al. (2009). The ER luminal binding protein (BiP) mediates an increase in drought tolerance in soybean and delays drought-induced leaf senescence in soybean and tobacco. J. Exp. Bot. **60:** 533–546.

Wang, D., Weaver, N.D., Kesarwani, M., and Dong, X. (2005). Induction of protein secretory pathway is required for systemic acquired resistance. Science **308:** 1036–1040.

Wei, J., Gaut, J.R., and Hendershot, L.M. (1995). In vitro dissociation of BiP-peptide complexes requires a conformational change in BiP after ATP binding but does not require ATP hydrolysis. J. Biol. Chem. **270:** 26677–26682.

Wei, J., and Hendershot, L.M. (1995). Characterization of the nucleotide binding properties and ATPase activity of recombinant hamster BiP purified from bacteria. J. Biol. Chem. **270:** 26670–26676.